

Probing Mott lobes via the AC Josephson effect

M.X. Huo¹, Ying Li¹, Z. Song^{1,*} and C.P. Sun^{2†}

¹*Department of Physics, Nankai University, Tianjin 300071, China and*

²*Institute of Theoretical Physics, Chinese Academy of Sciences, Beijing, 100080, China*

The alternating-current (AC) Josephson effect is studied in a system consisting of two weakly coupled Bose Hubbard models. In the framework of the mean field theory, Gross-Pitaevskii equations show that the amplitude of the Josephson current is proportional to the product of superfluid order parameters. In addition, the chemical potential–current relation for a small size system is obtained via the exact numerical computation. This allows us to measure the Mott lobes of the quantum phase transition.

PACS numbers: 03.65.Ud, 03.67.MN, 71.10.FD

Introduction. Recent development of experiments allows the detection of the quantum phase transition in strongly correlated many-body systems [1]. The relevant physics is captured by the Bose-Hubbard model, which describes the competition between the kinetic-energy and potential-energy effects. The Mott insulator (MI) to superfluid (SF) phase transition of the Bose-Hubbard model was described qualitatively using a mean field theory [2] and realized in a gas of ultracold atoms [3]. Generally, for the MI to SF transition, the superfluid order parameter predicted by the mean field theory can not be measured directly. However, in this letter, we propose a feasible realization to detect the phase transition and obtain the Mott lobes of the order parameter. The main idea relates to the well known alternating-current Josephson effect, which has been well investigated in the Bose-Einstein condensates (BEC) [4, 5, 6, 7].

The Josephson junction is composed of two superfluid parts separated by a tunnelling barrier. When a constant chemical potential difference is applied, the AC Josephson effect occurs, corresponding an oscillating particle flow through the barrier. If one part is fixed in superfluid state, the phase of other part should determine the amplitude of the AC current. Inversely, it is possible to detect the state of the target part via measuring the Josephson current across the barrier.

In this letter, through the well established mean field theory and spontaneous symmetry breaking mechanism for quantum phase transition, the analytical analysis reveals that the amplitude of the Josephson current is proportional to the product of superfluid order parameters of the two parts. Through the measurement of the AC Josephson current, the Mott lobes can be obtained indirectly. Moreover, numerical simulations show that the profile of the Mott lobes for small size system is consistent with that in thermodynamic limit. This opens a possibility to detect the BEC in small quantum device. As an application we discuss an experimental realization in a cavity-atom hybrid system based on the recent work in Ref. [8].

Hamiltonian and the mean field theory. The setup is

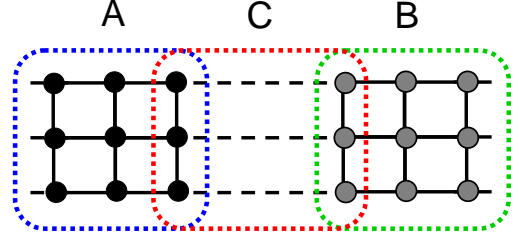


FIG. 1: (Color online) Schematic plot of the lattice model used in this work. (A) is a Bose-Hubbard model with the on site repulsion U triggering the Mott transition; (B) is a free boson lattice model with a chemical potential μ which controls the density of bosons in lattice A; (C) is a thin contact surface between A and B which can be represented by a direct weak tunnelling across A and B or a free boson lattice model with an on site repulsion larger than μ .

depicted as the following Hamiltonian

$$H = H_A + H_B + H_C, \quad (1)$$

where

$$\begin{aligned} H_A &= -\kappa \sum_{\langle i,j \rangle \in A} (a_i^\dagger a_j + h.c.) + \frac{U}{2} \sum_{i \in A} a_i^\dagger a_i^\dagger a_i a_i, \\ H_B &= -\kappa \sum_{\langle i,j \rangle \in B} (b_i^\dagger b_j + h.c.) + \mu \sum_{i \in B} b_i^\dagger b_i, \\ H_C &= -g \sum_{i \in C} (a_i^\dagger b_i + h.c.). \end{aligned} \quad (2)$$

Here a_i and b_i are the boson operators. In this paper, we consider lattices A and B having an identical structure with size N for simplicity. Each lattice site \mathbf{i} ($= 1, 2, \dots, N$) corresponds to two positions in lattices A and B, respectively. Among them, $\mathbf{i} \in C$ lies on the contact surface. We consider the weakly coupled case $g \ll \kappa$. Fig. 1 is a schematic representation of the setup.

We start our investigation from the mean field approximation. The order parameters can be defined as the expectation values of boson operators $a_i(t)$ and $b_i(t)$ in the Heisenberg picture by ignoring the fluctuations, i.e.,

$$\psi_{a,i}(t) \equiv \langle a_i(t) \rangle, \quad \psi_{b,i}(t) \equiv \langle b_i(t) \rangle, \quad (3)$$

where the average is taken with respect to the ground state. In this paper, we use a_i and b_i to denote the boson operators in the Schrödinger picture. In order to study the time evolution of the order parameter, we make use of the Gross-Pitaevskii (GP) equations in the lattice [9, 10]. The GP equations corresponding to the Hamiltonian (1) read

$$i\frac{\partial}{\partial t}\psi_{a,i} = -\kappa \sum_{\langle i,j \rangle} \psi_{a,j} + U |\psi_{a,i}|^2 \psi_{a,i} - g_i \psi_{b,i}, \quad (4a)$$

$$i\frac{\partial}{\partial t}\psi_{b,i} = -\kappa \sum_{\langle i,j \rangle} \psi_{b,j} + \mu \psi_{b,i} - g_i \psi_{a,i}, \quad (4b)$$

where $g_i = g$ for $i \in C$ and $g_i = 0$ for $i \notin C$.

When g is small enough, we can define solutions of Eqs. (4a) and (4b) as

$$\psi_{a,i} = \phi_a(t) \Phi_{a,i}, \quad \psi_{b,i} = \phi_b(t) \Phi_{b,i}, \quad (5)$$

where $\Phi_{a,i}$ and $\Phi_{b,i}$ are solutions for the ground states of Eqs. (4a) and (4b) when $g = 0$. $\Phi_{a,i}$ and $\Phi_{b,i}$ are set to be real and normalized as $\sum_i \Phi_{a,i}^2 = \sum_i \Phi_{b,i}^2 = 1$. Taking the periodic boundary condition, $\Phi_{a,i} = \Phi_{b,i} = 1/\sqrt{N}$. After replacing $\psi_{a,i}$ and $\psi_{b,i}$, GP equations (4a) and (4b) become the two-state model [11]

$$i\frac{\partial}{\partial t}\phi_a(t) = [E_a + U_a |\phi_a(t)|^2] \phi_a(t) - K \phi_b(t), \quad (6a)$$

$$i\frac{\partial}{\partial t}\phi_b(t) = E_b \phi_b(t) - K \phi_a(t), \quad (6b)$$

where

$$E_a = -2\kappa \sum_{\langle i,j \rangle} \Phi_{a,i} \Phi_{a,j} = -2d\kappa, \quad (7a)$$

$$E_b = \mu - 2\kappa \sum_{\langle i,j \rangle} \Phi_{b,i} \Phi_{b,j} = \mu - 2d\kappa, \quad (7b)$$

$$U_a = U \sum_i \Phi_{a,i}^4 = \frac{U}{N}, \quad (7c)$$

$$K = g \sum_{i \in A} \Phi_{a,i} \Phi_{b,i} = \frac{g}{N^{\frac{1}{d}}}, \quad (7d)$$

for two d -dimensional lattices with the periodic boundary condition and contact surface with size $N^{\frac{d-1}{d}}$. $\phi_{a,b}(t) = \sqrt{N_{a,b}} e^{i\theta_{a,b}}$ where $N_{a,b}$ and $\theta_{a,b}$ are the particle number and phase of the superfluid component in lattices A and B.

Substituting $\phi_{a,b}(t)$ into the above two-state model, we get

$$\frac{\partial z}{\partial t} = -2K \sqrt{1-z^2} \sin \Theta, \quad (8a)$$

$$\frac{\partial \Theta}{\partial t} = \Delta E + \Lambda z + \frac{2Kz}{\sqrt{1-z^2}} \cos \Theta, \quad (8b)$$

where $\Theta = \theta_a - \theta_b$, $z = (N_b - N_a)/(N_a + N_b)$, $\Delta E = E_b - E_a - \frac{U_a}{2} (N_a + N_b)$, and $\Lambda = U_a (N_a + N_b)/2$. Eqs.

(6a) and (6b) show that $N_a + N_b$ is conserved. Then the Josephson current (if the boson is neutral, the current corresponds to the flow of bosons) is

$$J(t) = \frac{\partial N_b}{\partial t} = -2K \sqrt{N_a N_b} \sin \Theta. \quad (9)$$

When $\mu \gg U, \kappa$, it becomes

$$J(t) = -\frac{2g\sqrt{N_a N_b}}{N^{\frac{1}{d}}} \sin \mu t. \quad (10)$$

Here $N_{a,b}$ is time-dependent. On the other hand, the upper bound of the particle immigration across the junction during a half period of oscillation, which corresponds to the case $N_{a,b} \sim N$, is of the order $\Delta N_b \sim g\sqrt{N_a N_b}/(\mu N^{\frac{1}{d}}) \sim gN^{\frac{d-1}{d}}/\mu$. For $N^{\frac{d-1}{d}} \ll N$, $N_{a,b}$ can be regarded as a constant, which corresponds to the order parameter defined in the framework of the mean field theory [2] as $\psi_\gamma \equiv \langle \gamma_i \rangle = \langle \gamma_i^\dagger \rangle = \sqrt{N_\gamma/N}$, ($\gamma = a, b$). Then the Josephson current is obtained as

$$J(t) = -2gN^{\frac{d-1}{d}} \psi_a \psi_b \sin \mu t. \quad (11)$$

Measurement of the order parameter. In this section, we focus on the experimental scheme to obtain the Mott lobes of the Bose-Hubbard model. It is based on measuring the magnitude and frequency component of the Josephson current. Our proposal for the measurement of the order parameter experimentally is as follows: (a) Parameters U , κ and μ are set to be values corresponding to a point $(\mu/U, \kappa/U)$ on the phase diagram, then cool the system to the ground state. (b) Take the ground state as an initial state, and shift the chemical potential to $\mu + \Delta\mu$ ($\Delta\mu \gg U, \kappa$). (c) Obtain the current $J(t)$ between A and B. (d) Numerically analyze the curve $J(t)$ to obtain

$$J_m(\mu/U, \kappa/U) = \max \{J(\mu/U, \kappa/U, t)\} \quad (12)$$

and the frequency component of the current from the formula

$$J(\mu/U, \kappa/U, \omega) = \sqrt{\frac{2}{\pi}} \int_0^\tau dt J(\mu/U, \kappa/U, t) \sin \omega t \quad (13)$$

as $\tau \rightarrow \infty$. (e) In the weak coupling limit $g \ll \kappa$, all the bosons in lattice B are in the superfluid state, i.e., $\psi_b \simeq \langle b_i^\dagger b_i \rangle^{1/2}$. Then ψ_b can be measured via the measurement of the average particle density in lattice B. (f) Construct the phase diagram $\psi_a(\mu/U, \kappa/U)$ according to Eq. (11).

Theoretically, the Josephson current arises from the time evolution of the superfluid state of the Hamiltonian (1). In this Hamiltonian, we add the chemical potential μ only in system B, but this is equivalent to adding a chemical potential $-\mu$ in system A, since adding a term $-\mu \sum_i (a_i^\dagger a_i + b_i^\dagger b_i)$ to the whole system

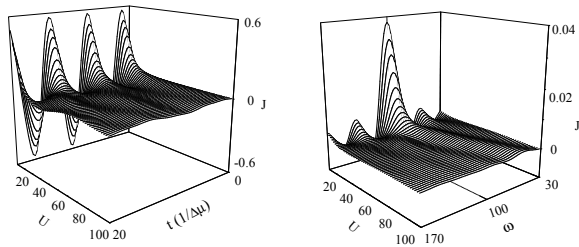


FIG. 2: (Color online) 3D plots of the Josephson current (a) $J(U, t)$ and its Fourier component (b) $J(U, \omega)$ for a small size system obtained by the exact diagonalization with $\kappa = 1$, $\Delta\mu = 100$, $g = 0.1$ and $\mu/U = 0.5$. In (b), the upper limit of the time integration is taken as $\tau(1/\Delta\mu) = 20$. As τ increases, the peak with frequency 100 will become higher and sharper. The current drops rapidly as U increases. These results show that the current is a Josephson alternating current with frequency $\Delta\mu$ and can be employed to witness the quantum phase transition.

does not bring any physical change. Then the order parameter of lattice A corresponds to the point $(\mu/U, \kappa/U)$ of the obtained phase diagram. At $t = 0$, the ground state of the Hamiltonian (1) is $|\varphi_g(\mu/U, \kappa/U)\rangle = |\varphi(0)\rangle$, which is the initial state for the time evolution driven by the Hamiltonian $H + \Delta\mu \sum_i b_i^\dagger b_i$, i.e., $|\varphi(t)\rangle = e^{-i(H + \Delta\mu \sum_i b_i^\dagger b_i)} |\varphi(0)\rangle$. Then the current across A and B is

$$J(\mu/U, \kappa/U, t) = -ig \sum_{i \in C} \langle \varphi(0) | \left(a_i^\dagger(t) b_i(t) - h.c. \right) | \varphi(0) \rangle, \quad (14)$$

where $a_i^\dagger(t)$ and $b_i(t)$ are boson operators in the Heisenberg picture. To demonstrate this scheme, the numerical simulation is performed for $N = 2$ system with $\kappa = 1$, $\Delta\mu = 100$, $g = 0.1$, and $\mu/U = 0.5$, which corresponds to a parallel line in the phase diagram of lattice A. Fig. 2(a) is the 3D plot of the Josephson current $J(U, t)$, which is a good sinusoidal curve vs time t when U is not very large, in which region systems A and B are both in the superfluid phase. When U is large enough, the amplitude of the current drops, which indicates that system A enters into the Mott insulating phase. Fig. 2(b) is the 3D plot of the Fourier component $J(U, \omega)$ obtained according to Eq. (13). The upper limit of the time integration (13) is taken as $\tau(1/\Delta\mu) = 20$. The larger values of τ will make the peak with frequency 100 higher and sharper. The current drops rapidly as U increases, which indicates the quantum phase transition of system A. These results show that the current is a Josephson alternating current with frequency $\Delta\mu$ and can be employed to witness the quantum phase transition.

According to the mean field results, when g is small enough, the Josephson current is proportional to the or-

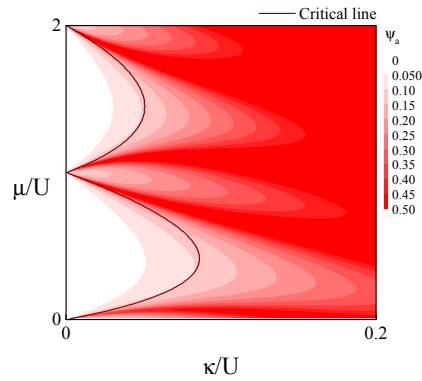


FIG. 3: (Color online) Mott lobes calculated by the exact diagonalization with an auxiliary field for a small size system (color contour map), and by the mean field method via the Gutzwiller trial wave function. The contour line denotes the boundary of two phases which corresponds to a vanishing order parameter. It is shown that although the result of the small system can not give the boundary of two phases, its contour lines are consistent with that from the mean field method in the thermodynamic limit very well.

der parameter of an isolated system with the Hamiltonian $H_A \rightarrow H_A - \mu \sum_i a_i^\dagger a_i$. However, the Mott lobes obtained in a finite size system from the above procedures (a-f) cannot be compared with the phase diagram obtained from the mean field method in the thermodynamic limit, which is usually obtained via the Gutzwiller trial wave function [2]. To compare the Josephson current with the mean field phase diagram, we need to develop another way to obtain the order parameter for a finite system in the framework of the spontaneous symmetry breaking. It is well known that the quantum phase transition is a consequence of U(1) symmetry breaking for an interacting boson system [12]. Then introducing an auxiliary field as

$$H_A - \mu \sum_i a_i^\dagger a_i \rightarrow H_A - \mu \sum_i a_i^\dagger a_i + \lambda \sum_i (a_i^\dagger + a_i) \quad (15)$$

breaks the U(1) symmetry breaking and induces the order parameter. Accordingly, the order parameter is determined by $\psi_a = \lim_{\lambda \rightarrow 0} \lim_{N \rightarrow \infty} \langle a_i \rangle$, where the average is taken for the ground state of the Hamiltonian (15). In the thermodynamic limit $N \rightarrow \infty$, the ground state $|\varphi_g^a\rangle$ is a coherent state and the vanishing ψ_a discriminates two phases. In this case, the order parameter is independent of λ . On the other hand, when lattice A is coupled to B, the order parameter obtained from Eqs. (11) and (14) should also be independent of g in the limit $N \rightarrow \infty$ and $g \rightarrow 0$.

In a finite system, although ψ_a obtained from the above two ways are not independent of λ and g , it is believed that their consistency should be revealed from the contour maps. To demonstrate this, the numerical simulation for a small size system is performed and compared

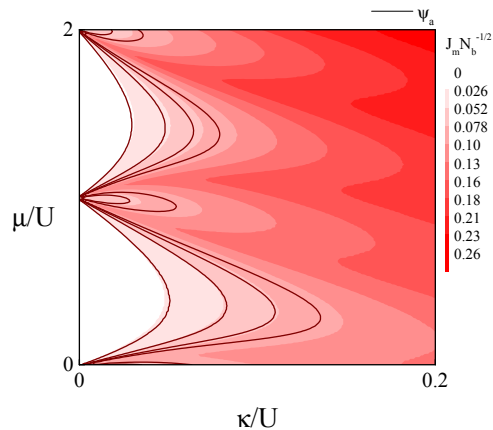


FIG. 4: (Color online) Mott lobes of the order parameter for a small size system calculated by the exact diagonalization with $\kappa = 1$, $\Delta\mu = 100$, and $g = 0.1$. The color contour map is obtained from the Josephson current, while the contour lines are obtained via an auxiliary field with $\lambda = 0.1$. It is shown that two results are consistent very well.

with the mean field method. Even for a small size system, the dimension of the Hilbert space of the Hamiltonian (15) is infinite. So the truncation approximation is taken for the exact diagonalization of the matrix for $N = 2$ and the average density $\langle a_i^\dagger a_i \rangle \in [0, 2]$. In Fig. 3, the Mott lobes calculated by the exact diagonalization with an auxiliary field for $N = 2$ system and by the mean field method via the Gutzwiller trial wave function are plotted. The contour line denotes the boundary of two phases, which corresponds to a vanishing order parameter. It is shown that although the result of the small size system can not give the boundary of two phases, its contour lines are consistent with that of the mean field method in the thermodynamic limit very well.

In Fig. 4, Mott lobes of the order parameter for a small size system are plotted through two different mechanisms with $\kappa = 1$ and $g = 0.1$. The color contour map is obtained from the Josephson current via the above procedures (a-f), while the contour lines are obtained from the Hamiltonian (15) by the exact diagonalization. It is shown that two results are consistent very well, which indicates that the property of the small size system can shed light on the profile of Mott lobes in the thermodynamics limit.

Discussion. In order to detect the Mott lobes of the quantum phase transition, we investigate the AC Josephson effect in a system consisting of two weakly coupled Bose-Hubbard models. The mean field theory in the thermodynamic limit and the numerical simulation for a small size system show that, through measuring the magnitude and frequency component of the Josephson current, the Mott lobes can be measured.

To realize this scheme experimentally, as mentioned

before, a good candidate is the coupled cavity system with each cavity interacting with 4-level atoms driven by an external laser [8]. In this system, the repulsion U can indeed be strong enough to observe the Mott insulator state for photons. Moreover, according to Refs. [8] and [13], the controllable range of the chemical potential required by our scheme is in experimentally accessible parameter regimes. In fact, in such an effective Bose-Hubbard system, the on-site interaction U and chemical potential μ for photons are determined by

$$U = S \left(\frac{g_{13}}{\Omega} \right)^2 \frac{g_{24}^2}{\Delta}, \quad \mu = S \left(\frac{g_{13}}{\Omega} \right)^2 \epsilon, \quad (16)$$

under the conditions $g, \Delta, g_{24}, \epsilon \ll \Omega$; $g_{24}g \ll |\Delta\Omega|$. Here Ω is the Rabi frequency of the driving laser; S is the atom number in each cavity; g_{13}, g_{24} are the couplings between cavity mode to the atomic levels; δ, Δ and ϵ are detunings of atomic transitions with respect to the cavity and laser fields. All the notations are identical with those used in Fig. 1 of Ref. [8].

By fixing $S (g_{13}/\Omega)^2$ and adjusting g_{24}^2/Δ and ϵ, U and μ are tunable independently. This allows us to simulate the Hamiltonian (2) by setting $\epsilon = 0$ in lattice A to get $\mu = 0$, and $g_{24} = 0$ in lattice B to get the vanishing U . Subsequently, to drive the quantum phase transition and probe the Mott lobes of lattice A, the parameters in two systems A and B are tuned according to the procedures (a-f). In this scheme, the Josephson current $J(t)$ is the flow of photons in photonic crystal waveguides, which can be imaged via a high-resolution imaging technique, the collection scanning near-field optical microscope [14]. This predicts that the Mott lobes for a small quantum device can be detected experimentally.

This work is supported by the NSFC with grant Nos. 90203018, 10474104 and 60433050, and NFRPC with Nos. 2006CB921206 and 2005CB724508.

* Electronic address: songtc@nankai.edu.cn

† Electronic address: suncp@itp.ac.cn;
URL: <http://www.itp.ac.cn/~suncp>

- [1] I.B. Mekhov *et al.*, Nature **3**, 319 (2007)
- [2] M.P.A. Fisher *et al.*, Phys. Rev. B **40**, 546 (1989).
- [3] M. Greiner *et al.*, Nature **415**, 39 (2002).
- [4] F.S. Cataliotti *et al.*, Science **293**, 843 (2001).
- [5] S. Giovanazzi, A. Smerzi and S. Fantoni, Phys. Rev. Lett. **84**, 4521 (2000).
- [6] M. Albiez *et al.*, Phys. Rev. Lett. **95**, 010402 (2005).
- [7] S. Levy *et al.*, Nature **449**, 579 (2007).
- [8] M.J. Hartmann and M.B. Plenio, Phys. Rev. Lett. **99**, 103601 (2007).
- [9] F. Dalfovo *et al.*, Rev. Mod. Phys. **71**, 463 (1999).
- [10] A. Polkovnikov *et al.*, Phys. Rev. A **66**, 053607 (2002).
- [11] A. Smerzi *et al.*, Phys. Rev. Lett. **79**, 4950 (1997).
- [12] S. Sachdev, *Quantum Phase Transition*, (Cambridge University Press, Cambridge, 1999).

- [13] D.K. Armani *et al.*, Nature (London) **421**, 925 (2003); T. Aoki *et al.*, Nature (London) **443**, 671 (2006); S.M. Spillane *et al.*, Phys. Rev. A **71**, 013817 (2005).
- [14] S.I. Bozhevolnyi *et al.*, Phys. Rev. B **66**, 235204 (2002).